



Morphological and genetic identification and isotopic study of the hair of a cave lion (*Panthera spelaea* Goldfuss, 1810) from the Malyi Anyui River (Chukotka, Russia)



O.F. Chernova^{a,*}, I.V. Kirillova^b, B. Shapiro^{c,d}, F.K. Shidlovskiy^b, A.E.R. Soares^c, V.A. Levchenko^e, F. Bertuch^e

^a Severtsov Institute of Ecology and Evolution, Russian Academy of Sciences, Leninskii pr. 33, Moscow 119071, Russia

^b Ice Age Museum, "National Alliance of Shidlovskiy "Ice Age", 119 Bld, Mira pr, Moscow 129223, Russia

^c Department of Ecology and Evolutionary Biology, University of California Santa Cruz, 1156 High Street, Santa Cruz, CA 95064, USA

^d UCSC Genomics Institute, University of California Santa Cruz, 1156 High Street, Santa Cruz, CA 95064, USA

^e Australian Nuclear Science and Technology Organization, Locked Bag 2001, Kirrawee DC, NSW 2232, Australia

ARTICLE INFO

Article history:

Received 9 November 2015

Received in revised form

4 April 2016

Accepted 17 April 2016

Available online 29 April 2016

Keywords:

Ancient DNA

Cave lion

Chukotka

Hair

Ice Age

Isotopes

AMS radiocarbon dating

SEM

ABSTRACT

We present the first detailed analyses of the preserved hair of a cave lion (*Panthera spelaea* Goldfuss, 1810). The hair was found in association with a skeleton that was recovered recently from perennially frozen Pleistocene sediments in the lower reaches of the Malyi Anyui River (Chukotka, Russia). We extract mitochondrial DNA from the hair to confirm its taxonomic identity, and perform detailed morphological analyses of the color and structure of the hair using light optical microscopy and SEM. In addition, we compare the cave lion hair to hair taken from the back and mane of an African lion. We find that cave lion hair is similar but not identical to that of the present-day lion. In addition to slightly different coloration, cave lions had a very thick and dense undercoat comprising closed and compressed wavy downy hair with a medulla. In addition, while the microstructures of the medulla and cortex of cave lion hair are similar in extinct and living lions, the cuticular scales of cave lion hair are higher than those in living lions, suggesting that cave lion hair is stronger and more robust than that of living lions. We hypothesize that the differences between cave lion hair and present-day lion hair may be due to adaptations of cave lions to the harsh climatic and environmental conditions of the Pleistocene Ice Ages.

© 2016 Elsevier Ltd. All rights reserved.

1. Introduction

The cave lion *Panthera spelaea* Goldfuss, 1810, is among the most iconic representatives of the Ice Age megafauna. During the Pleistocene, the cave lion range extended from Western Europe into North America, and fossils are found throughout this distribution. Studies of these fossils and of depictions of cave lions in Paleolithic art have provided considerable insights into the cave lion's diet and appearance, and recent genetic analysis confirmed their evolutionary affinity with present-day large cats (Vereshchagin, 1971; Kurten, 1985; Turner, 1997; Baryshnikov and Boeskorov, 2001; Sotnikova and Nikolsky, 2006; Diedrich, 2008, 2011; Barnett et al., 2009; Wheeler et al., 2009; Bocherens et al., 2011; Diedrich

and Rathgeber, 2011). However, until recently, mummified remains of cave lions had never been recovered, and little was known coloration or other attributes that can be learned only from the study of preserved hair and soft tissues.

In Russia, remains of cave lions are geographically widespread but rare. In 2008, a resident of a settlement on the Malyi Anyui River, Western Chukotka (Fig. 1A), discovered an incomplete skeleton of a cave lion preserved in perennially frozen permafrost soils (Kirillova et al., 2015). A distinctive feature of this discovery was the presence of keratin derivatives of the skin — a claw sheath and hair (Kirillova et al., 2015). While identification of the claw was not in doubt, this was the first discovery of presumed cave lion hair and, owing to a lack of comparative data, it was not possible to confirm the taxonomic identity of the hair.

At the time of discovery of the Malyi Anyui cave lion, descriptions of cave lion hair were known only from Paleolithic Art. Based on these cave drawings (Fig. 1B), cave lions probably had

* Corresponding author.

E-mail address: olga.chernova.moscow@sevin.ru (O.F. Chernova).

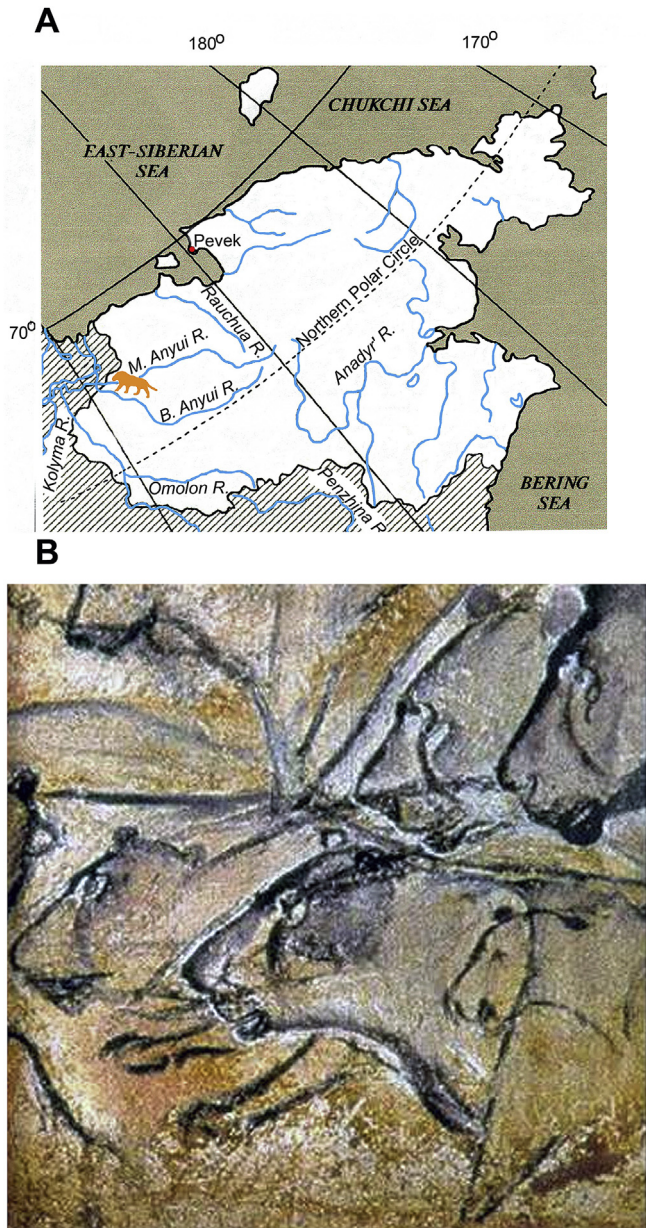


Fig. 1. Map showing the locality of the cave lion skeleton and fur find (A) and replica of the cave lion pictogram in the Chauvet Cave (France) (B) (after Arduini and Teruzzi, 1993).

monochromatic yellow-brown fur, no mane, and a tail that ended with a brush of hair at the tip, similarly to present-day African lions (*P. leo leo* Linnaeus, 1758) (Arduini and Teruzzi, 1993; Packer and Cluttons, 2000; Nagel et al., 2003; Yamaguchi et al., 2004). Previous work to characterize the hair of present-day lions was performed by Chakraborty et al. (1996), who provided a description of color and configuration, morphological metric data, and microstructure (using light optical microscopy) of guard hairs in the back of Asiatic lion (*P. leo persica* A.B. Meyer, 1826) (Chakraborty et al., 1996), and by Chernova et al. (2011), who presented photomicrographs of the main layers of African lion hair. Here, we confirm the taxonomic identity of the newly discovered cave lion hair using a comparative mitochondrial DNA analysis and assess diet using isotopic analysis. We also use scanning electronic microscopy (SEM) to characterize the degree of similarity between hair from a cave lion and a present-day African lion. We identify several

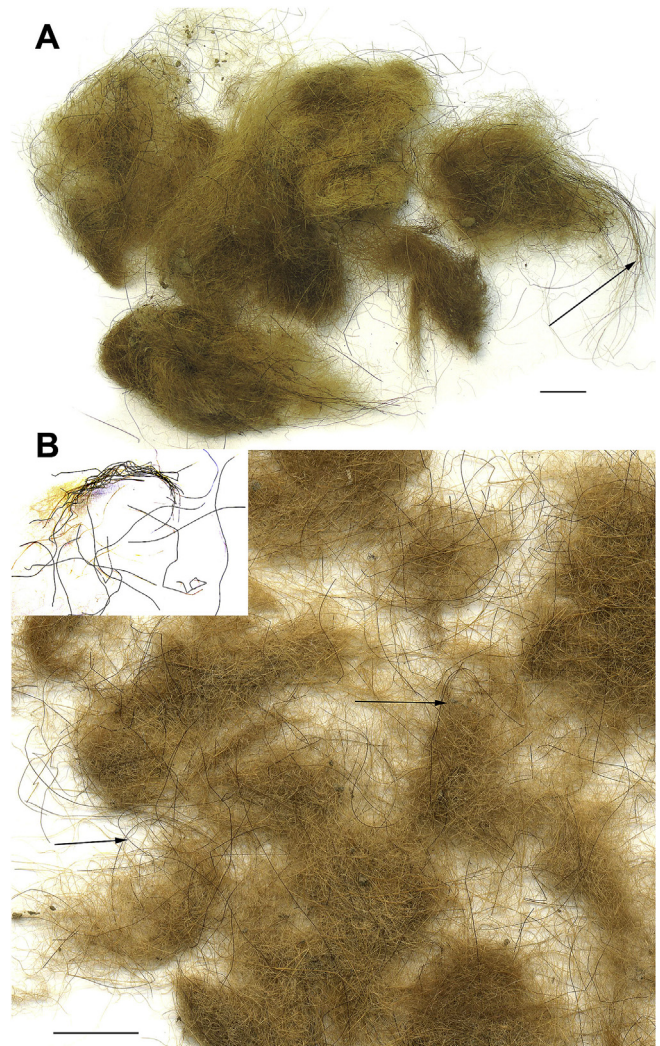


Fig. 2. Photomicrographs of the yellowish matted fur found alongside the remains of a skeleton of cave lion. (A) Small wads of fur with black guard hairs indicated by arrows; (B) the hair was highly heterogeneous: thick black guard hairs and thin and wavy yellowish downy hairs are visible, and black guard hairs are indicated by arrows; (Box) guard hairs. Scale bars are 1 cm. *Note:* In the cave lion fur we found one dark hair (thickness up to 34 μm) identified as a small rodent hair. (For interpretation of the references to color in this figure legend, the reader is referred to the web version of this article.)

differences between the two lions that we hypothesize arose as a consequence of adaptations of cave lions in their Ice Age environment.

2. Material

We discovered several compact wads of hair among a variety of fossil remains (67 items) 14 km upstream of Anuisk (68.18° N, 161.44° E) in a steep riverbank (Fig. 1A) below water level. This discovery was noted previously (Kirillova et al., 2015), but has not yet been thoroughly described.

The hair samples recovered from the site were of yellowish and matted fur that formed loose wads mostly comprised of thin, wavy, downy hair of the undercoat and longer, thicker, darker and tough guide hair of the overhair (Fig. 2A and B, the box). For detailed analyses, we selected a wad of hair with a diameter of around 7 cm, and a weight of approximately 5 g (collection number F-2678/70). This and remaining material is stored in the Ice Age Museum

Table 1

Accession numbers for the sequences used in the phylogenetic reconstruction of the gene CYTB for the big cats *Panthera leo* spp. and the domestic cats *Felis catus*.

Species, subspecies	Common name	Accession number
<i>Panthera leo leo</i>	African Lion	KM374707.1
<i>P. leo leo</i>	African Lion	KC495955.1
<i>P. leo leo</i>	African Lion	KM374704.1
<i>P. leo leo</i>	African Lion	NC_020677.1
<i>P. leo leo</i>	African Lion	KJ652247.1
<i>P. leo persica</i>	Asiatic Lion	NC_018053.1
<i>P. leo persica</i>	Asiatic Lion	JQ904290.1
<i>P. leo persica</i>	Asiatic Lion	KC834784.1
<i>P. leo spelaea</i>	Cave Lion	KC701375.1
<i>P. leo spelaea</i>	Cave Lion	KC701376.1
<i>P. onca</i>	Jaguar	HM107682.1
<i>P. pardus</i>	Leopard	JF720063.1
<i>Felis catus</i>	Domestic Cat	AB004237.1
<i>F. catus</i>	Domestic Cat	AB004238.1

(National Alliance of Shidlovskiy “Ice Age”), Russia. Two small samples of the cave lion hair were used for genetic analysis, which was performed in the dedicated ancient DNA facility at the Paleogenomics Laboratory of the University of California Santa Cruz. In addition, samples of the claw sheath (OZQ2910) and fur (OZQ292) were sent to the Australian Nuclear Science and Technology Organisation for dating via radiocarbon accelerator mass spectrometry (AMS) and associated isotopic analyses.

Finally, we studied in detail the morphology of a total of 30 strands of cave lion hair. For morphological analysis, hair is subdivided into two main categories, guard hair and downy hair, and to several subcategories (orders) within these two main categories. Guard hair makes up the top coat, and downy hair, of which many strands grow from the same follicle and surround guard hair, makes up the undercoat. The orders of guard and downy hair subdivide them by color and structure. We collected five strands each of different categories and orders of hair from the cave lion, representing four orders of guard hair and two orders of downy hair. For comparison to the cave lion hair, we collected 40 strands of hair

from the mane and back of a 10-year-old adult male African lion, Miron, from the Moscow Zoo, which was provided to us by Moscow Zoo superintendents. These 40 strands represented two orders of guard hair from the mane and four orders of guard hair and two orders of downy hair from the back of the African lion.

3. Methods

3.1. Ancient DNA extraction and sequencing

For two small subsections of cave lion hair, we performed DNA extraction and library preparation using standard protocols for ancient DNA extraction and sequencing (Shapiro and Hofreiter, 2012) in a dedicated sterile facility at UC Santa Cruz. Briefly, we extracted DNA using the protocol described by Dabney et al. (2013), with the modifications suggested by Campos and Gilbert (2012). We then prepared an Illumina DNA sequencing library following Meyer and Kircher (2010), where the libraries were cleaned between each step using Sera-Mag SPRI SpeedBeads (Thermo-Scientific) in 18% PEG-8000. We sequenced the resulting libraries using a MiSeq Illumina sequencer with v3 kits, and processed the resulting sequencing data by removing adapters and merging reads including a minimum overlap of ten base-pairs between forward and reverse reads using SeqPrep (<http://github.com/jstjohn/SeqPrep>). We mapped the merged reads against the *P. leo persica* mitochondrial genome (GenBank accession NC_018053.1) using MIA (<http://github.com/udo-stenzel/mapping-iterative-assembler>). We aligned the assembled regions against known *P. leo spelaea* sequences for the mitochondrial genes ATP synthase protein 8 (ATP8) and Cytochrome B (CYTB), which we downloaded from GenBank (<http://www.ncbi.nlm.nih.gov>).

3.2. Radiocarbon age determination and isotopic study

We analysed the isotopic composition of hair and claw samples at the Joint Usage Centre at the Institute of Ecology and Evolution RAS, Moscow. Aliquots were cleaned by degreasing with alcohol

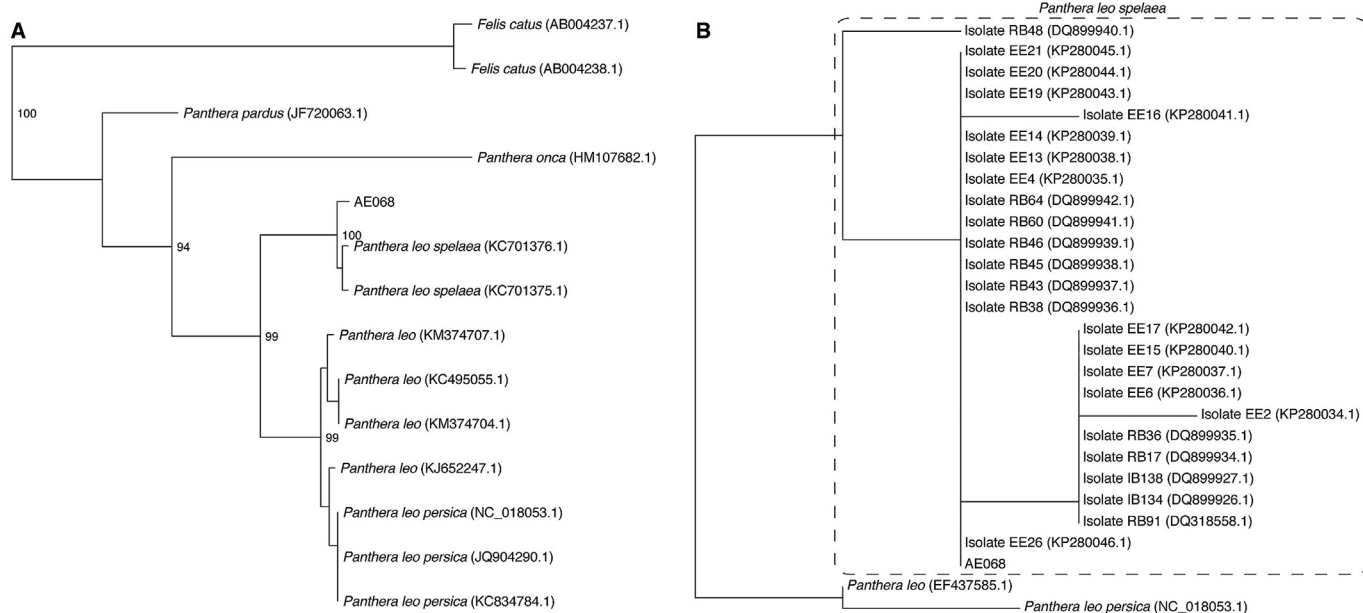


Fig. 3. Phylogenetic trees showing the (A) evolutionary relationships among members of the *Panthera* genus based on the CYTB gene, using maximum likelihood estimates under the HKY + G model with 500 bootstrap replicates; and a (B) similar maximum likelihood estimate for the ATP8 gene of the Cave, African, and Asiatic lions. GenBank accession numbers for all samples are provided in Table 1.

Table 2
Carbon and nitrogen isotope results for samples OZO291 (the claw) and OZQ292 (the hair) of the cave lion *Panthera spelaea*.

Sample	OZ number	Client ID	C:N (atomic)	$\delta^{13}\text{C}$ bulk	$\delta^{13}\text{C}$ graphite	$\delta^{15}\text{N}$	^{14}C , pMC
Claw	Q291	S-3-F-2678/66	3.6	-21.2 ± 0.2	-20.6 ± 0.2	11.7 ± 0.1	0.00 ± 0.01
Hair	Q292	S-4-F-2678/70		-21.4 ± 0.3	-19.5 ± 0.2	12.1 ± 0.05	2.81 ± 0.05

following by a thorough wash with distilled water, after which they were allowed to air dry. We performed measurements of keratin composition on a Thermo-Finnigan Delta V Plus continuous flow IRMS coupled with an elemental analyzer (Thermo Flash 1112), as described elsewhere (Kirillova et al., 2015). Radiocarbon AMS dating was performed at the Australian Nuclear Science and Technology Organisation (ANSTO). There, samples OZQ291 (claw) and OZQ292 (wool/hair) were treated following the O'Connell and Hedges (1999) protocol to remove possible contamination. The samples were subjected to ultra-sonication first in deionized water, then twice in a mixture of methanol and chloroform, and finally three times in deionized water. The samples were then treated with 2 M HCl at room temperature for 2 h to remove any carbonate contamination, rinsed with deionized water and freeze-dried. A subsample of claw material (hair was not used for this step due to the limited amount of sample available) was analysed for C:N ratio and stable isotopes on an EA Elementar-Vario Micro coupled to a Isoprime IRMS. Results were normalised to Acetanilide (N % = 10.36). A commercially certified reference standard from Elemental Microanalysis Ltd. (High Organic Sediment Standard OAS, No. B2151), with N = 0.50%, was processed along with the claw sample as a standard. For radiocarbon dating, both claw and hair samples were turned into graphite following Hua et al. (2001). Graphite targets were analysed for radiocarbon using the STAR AMS 2 MV Tandemron (Fink et al., 2004). Graphite that was left over after AMS measurements was used for $\delta^{13}\text{C}$ determination on an Isoprime IRMS, as required for radiocarbon isotopic fractionation correction.

3.3. Light optical microscopy and morphological analyses

Using a binocular microscope, we divided both the ancient hair and that of the living lion into different categories, based on the thickness and configuration of the hair shafts. We identified two main categories of hairs, guard hairs and downy hairs, and further subdivided these into several orders within each category. We measured the shaft and medullar thickness of each hair under an Amplival light microscope (VEB Carl Zeiss, Jena), a Leica DMLS microscope with a digital video camera (Germany) using a $\times 10$ eyepiece and $\times 10$, $\times 40$, and $\times 63$ lenses, and a motorized Keyence Biorevo BZ-9000 microscope (Japan). The largest of the guard hairs were studied under JSM 840A (Japan) and TESCAN (Czech Republic) scanning electron microscopes (SEM). To prepare the samples for SEM, each strand of hair was washed and degreased with shampoo and then washed in distilled water, and then dehydrated in ethanol of increasing concentration. We obtained longitudinal and transversal (cross) sections using a sharp razor blade, and fixed each section on stubs with clear nail polish. We coated the samples in an Edwards S-150 A (UK) gold sputter, and then viewed and

photographed them in the accelerating voltage of 15 kV.

We made electronic graphs from longitudinal and cross-sections of the base and the mid-length of the hair shafts, and from the cuticle surface along the shaft from the base to the mid-length of shaft and to the top at magnifications $\times 200$, $\times 300$, $\times 450$, $\times 600$, $\times 700$, $\times 800$. Because many of the preserved strands of hair that were recovered were broken toward the tip, we focus our morphological analysis on the lower two thirds of the hair, from the base to the mid-shaft. We then made photomicrographs representing these same components of the hair: the cross sections of a single hair; the mid-length of the shaft of amplified hair; medulla and cortex in a cross section of a hair; and prints of the cuticle ornament. In addition, we studied the hair 'disks', which are specific keratinous compartments of medulla that appear as the medulla breaks up under the alkaline thermal hydrolysis (Kisin, 2001). To create these disks, we performed thermal chemical hydrolysis: we placed the hair fragments in a 10–15% solution of NaOH and maintained them at a temperature of 50–90 °C for maceration; in some cases, further maceration led to the disintegration of the discs on groups of keratinous 'cells'. Using standard methods for SEM (Sokolov et al., 1988), we produced images of cross-sections of different parts of the hair shaft, medulla and cortex on the transversal and longitudinal sections of a hair. These images provide details of the configuration of the hair shaft (based on its width), the peculiarities of cortex pigmentation, the topology and degree of development of the medulla, and the microstructure of the hair.

4. Results

4.1. Genetic identification

Of the two samples processed for preserved DNA, only one provided sufficient quantities of DNA for analysis. For this sample (AE068), we performed taxonomic identification by we assembling two mitochondrial loci, ATP8 and CYTB, as these had been isolated previously from cave lions. For ATP8, AE068 was identical to cave lions belonging to Haplogroup I as described in Ersmark et al. (2015), which includes Siberian and European specimens ranging in age from 37 to 62 kyrs (Ersmark et al., 2015). Because CYTB is known to be more variable among felids, following mapping, we created an alignment of CYTB sequences that included other members of the *Panthera* genus plus *Felis catus* (Table 1) using MUSCLE (Edgar, 2004).

We inspected the alignment visually in SeaView v.4.5.4 (Gouy et al., 2010) and constructed a maximum likelihood phylogenetic tree using PhyML 3.0 as implemented in SeqView v.4.5.4 (Guindon et al., 2010). We used a HKY + G model, as suggested by jModelTest v.2.1.4 (Darriba et al., 2012), with 500 bootstrap replicates. The

Table 3
Radiocarbon age determination of the fur sample of the cave lion *Panthera spelaea*.

ANSTO code	Sample type	Submitted ID	$\delta^{13}\text{C}$ per mil			Percent modern carbon			Conventional ^{14}C age		
			$\delta^{13}\text{C}$		1 σ error	pMC		1 σ error	yrs BP		1 σ error
OZQ292	Hair/wool	S-4F-2678/70	-19.5	\pm	0.2	2.81	\pm	0.05	28,690	\pm	130

Table 4Some morphological features cave lion, *Panthera spelaea*, and African lion, *P. leo leo*, hair.

Species/subspecies, sample	Category, order	Color	Shaft configuration	Length, mm, min–max, n = 5	Width, μ m, min–max, n = 5	Medulla topography	Medulla width, % of shaft width, min–max, n = 5
<i>Panthera spelaea</i> , topography of the sample is unknown	Guard hair (GH) I	Black	Straight, cylindrical, without local thickening ('granna')	Fragments, 45–50	180–200	In the median part of the shaft	75–80
	GH II	Dark-brown	The same as the above cell, and with a slight ring in the lower third of shaft	Fragments, 35–40	79–90		60–70
	GH III	Lower part of a shaft is dark-brown, upper part is light-yellow	Weakly waved	Hereinafter: the entire hair, 56–60	57–68	Moved in the direction of a lesser curvature of the shaft wave	55–50
	GH IV Downy hair (DH) I	Light-yellow, whitish	Waved	30–35	43–45 23–45		40–45 25–30
<i>P. leo leo</i> , mane	DH II	In the median part of the shaft		29–35	17–23		23–25
	GH I	Black, dark-brown, with narrow yellow ring on the upper part of a hair, and with a black tip	Straight, cylindrical, a bit flattened, without a granna, and waved in a shaft base	150–157	113–124	In the median part of the shaft	60–66
Back	GH II	The same as the above cell, and with wide yellow ring		54–56	79–85		59–60
	GH I	The same as the above cell, and with narrow yellow ring around the median part of the shaft and black tip	Straight, cylindrical, with a slight thickness in light ring	33–35	96–113		70–80
	GH II	Light-yellow, with whitish ring, and without black tip		29–30	79–113		59–60
	GH III			27–28	68–90		48–50
	GH IV			23–25	32–34		43–45
	DH I DH II	Whitish	Straight, cylindrical, slightly flattened	3.2–3.5 3–3.1	23–28 11–17		28–30 Fragmental

resulting tree show strong statistical support for AE068 within the clade that includes previously published *P. leo spelaea* sequences (Fig. 3).

4.2. Isotopic study and AMS radiocarbon dating

Stable isotope results for the hair and claw sheath show good agreement both with each other and with previous determinations for bones (Kirillova et al., 2015) (Table 2). The $\delta^{15}\text{N}$ isotope signature indicates that the fur and claw belonged to a predator with a largely carnivorous diet.

The C:N ratio of the preserved keratin lies within the normal range, indicating that the preservation of the material was acceptable for dating. The keratin, as expected (O'Connell et al., 2001), exhibited a slightly higher C:N ratio than the collagen from associated bones (Kirillova et al., 2015). The carbon stable isotope ratios of the graphite targets showed little fractionation in processing, and agreed well with bulk samples measurements.

The AMS radiocarbon dates generated from the hair provided a significantly younger age than that for the associated skeleton (Table 3). Previously, radiocarbon dates for both a rib and the horny claw sheath were shown to be beyond the limits of this method (>61,000 years; Kirillova et al., 2015). Radiocarbon dating analysis of the fur, however, provided an uncalibrated ^{14}C age of $28,690 \pm 130$ years. While these results complicate the attribution of the fur to the skeleton, we note that, given the well-developed medulla in the cave lion hair, there is a chance that the standard protocol to clean the hair was unable to completely remove contaminants that may have been trapped within the medullar cavities. Such contamination may explain the difference in the recovered radiocarbon dates. Future work, potentially including the application of a modified ABA treatment that may avoid complete dissolution of the hair sample (Richardin et al., 2011), will be necessary to resolve this inconsistency in dating.

4.3. Morphological and comparative analyses of lion hair

4.3.1. Differentiation, coloration, configuration and size

We subdivided the hairs into two major categories: guard hair (GH, I–IV orders) and downy hair (DH, I–II orders), based on the maximum length, thickness, and configuration of the shaft. Many GH were preserved with broken tips; for these, we used only profile and maximum thickness to designate their order (Table 4). Color of GH varies from yellowish to dark-brown, without a black tip. DH are yellowish or whitish.

4.3.1.1. The cave lion. GH I are typically primary hairs, up to 50 mm in length. They are long, black, thick, strong, and smooth, without sharp bulges. The base of the shaft is cylindrical but becomes flattened on one side by the mid-length of the hair (Fig. 4A–C). The medulla is well developed and occupies up to 80% of the width of the shaft (Fig. 4A).

GH II are also dark, with cylindrical shafts and a slight wave in the lower third of the shaft. The thickness of each hair varies from 79 to 90 μ m, and the medulla is not as developed as that of GH I (Table 4).

GH III have a weakly waved shaft. They are bi-colored: the upper half of a shaft is light yellow and the lower part is dark-brown. GH III are 60 mm in maximum length and thinner than GH I–II, and contain a medium developed medulla (Table 4). In wavy portions of the shaft, the medulla is shifted toward the direction of lesser curvature, which distinguishes GH III from other GH I–II.

GH IV are thinner (45 μ m) than GH I–III, but all other features are the same as for GH III (Table 4).

DH are yellowish or whitish, long (up to 30–35 mm when stretched out), and curly, with shafts that are characterized by three to six waves, giving them the appearance of elastic springs (Fig. 5A, box). Because they are more numerous than GH, DH provide the bulk of the thick mass of hair. In the wave, the thickness of DH I

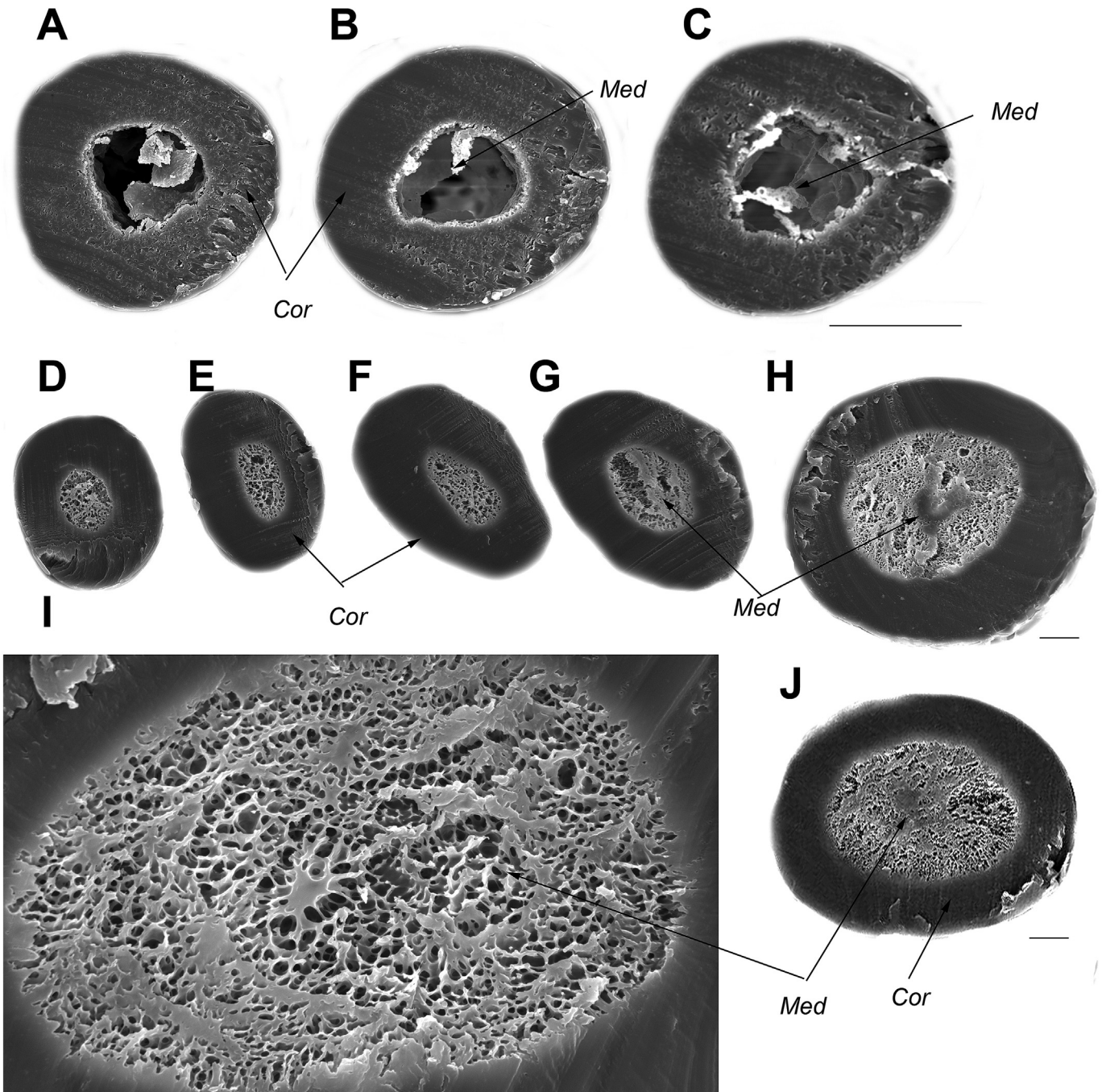


Fig. 4. SEM results showing microstructure of the guard hair of cave lion (A, B, C) and the present-day African lion (D–J) on cross-sections of the hair shaft. (A) base of the shaft; (B) above a base of the shaft; (C) mid-length of the shaft; (D–H) sequentially along the shaft from a base to a mid-length of the hair from the back; (I) the medulla; (J) mid-length of a hair from the mane; *Cor* = cortex; *Med* = medulla. Scale bars are: A, B, C — 100 μm ; D, E, F, G, H, I, J — 10 μm .

reaches 45 μm , but between waves they are not more than 23 μm thick. The medulla is shifted in the direction of a lesser curvature of the wave and takes up to 30% of the thickness of the shaft.

DH II are up to 23 μm thick, with a medulla that is shifted in the direction of the smaller curvature of the wave, where it is either fragmented or takes up to 25% of the thickness of the shaft (Table 4).

4.3.1.2. The African lion. In our analysis of the African lion *mane* we identified GH I and II of similar configuration but different in length and thickness of the shaft than in the cave lion. African lion GH I

and II are dark-brown or almost black, with more intense colors in GH I than GH II. They are banded with a yellowish ring in the upper third of the shaft; this ring is wider in GH II and becomes dark-brown at the tip of the hair. The shafts of GH I and II are right cylindrical or slightly flattened (Fig. 3J), and have a sinuous curve in the lower third. They reach 157 mm in length for GH I and 56 mm for GH II, with a maximum diameter of 124 and 85 μm , respectively. The medulla takes up to 60–66% of the thickness of shaft (Table 4).

DH were not found in the mane sample.

All categories and orders of hair were found on the *back* of the

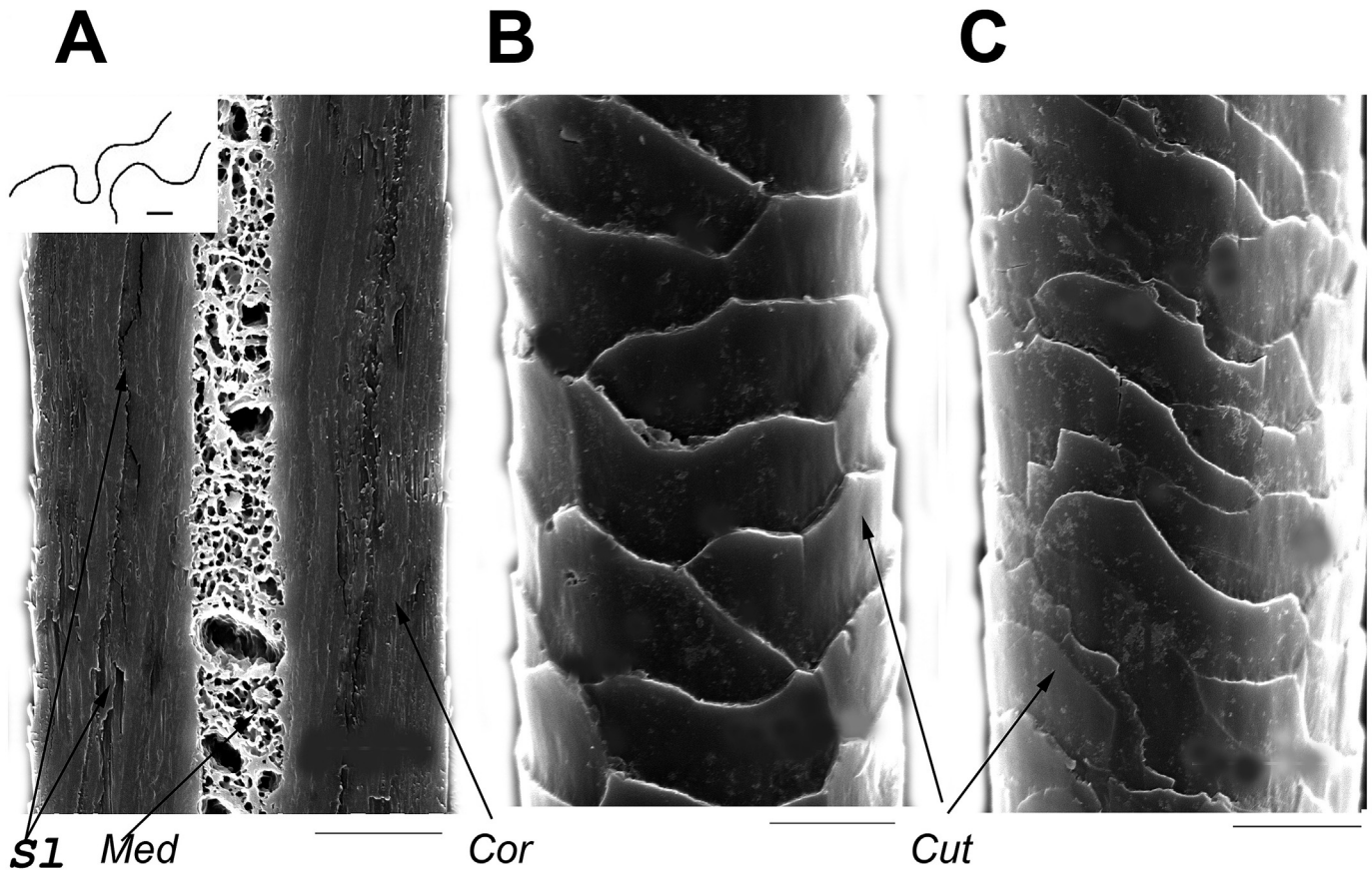


Fig. 5. SEM results showing microstructure of the downy hair of cave lion. (A) the medulla of the mid-length of shaft in a longitudinal section; (box) photomicrograph of the shaft configuration; (B) the cuticular patterns of base of the shaft; (C) the same of the mid-length of the shaft; *Cor* = cortex; *Cut* = the cuticular scale; *Med* = medulla; *S1* = longitudinal slit. Scale bars are: A, B, C — 10 μm ; box — 5 μm .

African lion. All are flexible and have a straight cylindrical shaft without undulating curves. The color is similar to that of the lion's mane but less intense. A light ring is apparent in the upper third of the shaft, and this ring is wider on GH II, where it occupies almost a third of the shaft. GH III and IV are yellowish in color and with thickened, whitish shafts in the area of the light ring. GH I and GH II are similar in width to cave lion GH I (Table 4). GH III and IV are distinguished by their smaller lengths (Table 4). In GH III and IV, the medulla is located strictly in the mid-length of the shaft and its configuration matches that of the shaft (Fig. 4D, E, F, G, H). The medulla has medium development (40–50% of the thickness of the shaft) in the mid-length of the hair, but thickens in the light ring, becoming up to 60–80% of the thickness of GH I and II.

DH are whitish without a light ring, almost not wavy, and do not exceed 17 μm in thickness. They differ from cave lion DH in the degree of medullar development, which ranges from making up 30% of the thickness of the shaft (DH I) to being highly fragmented (DH II) (Table 4). Wavy DH are absent.

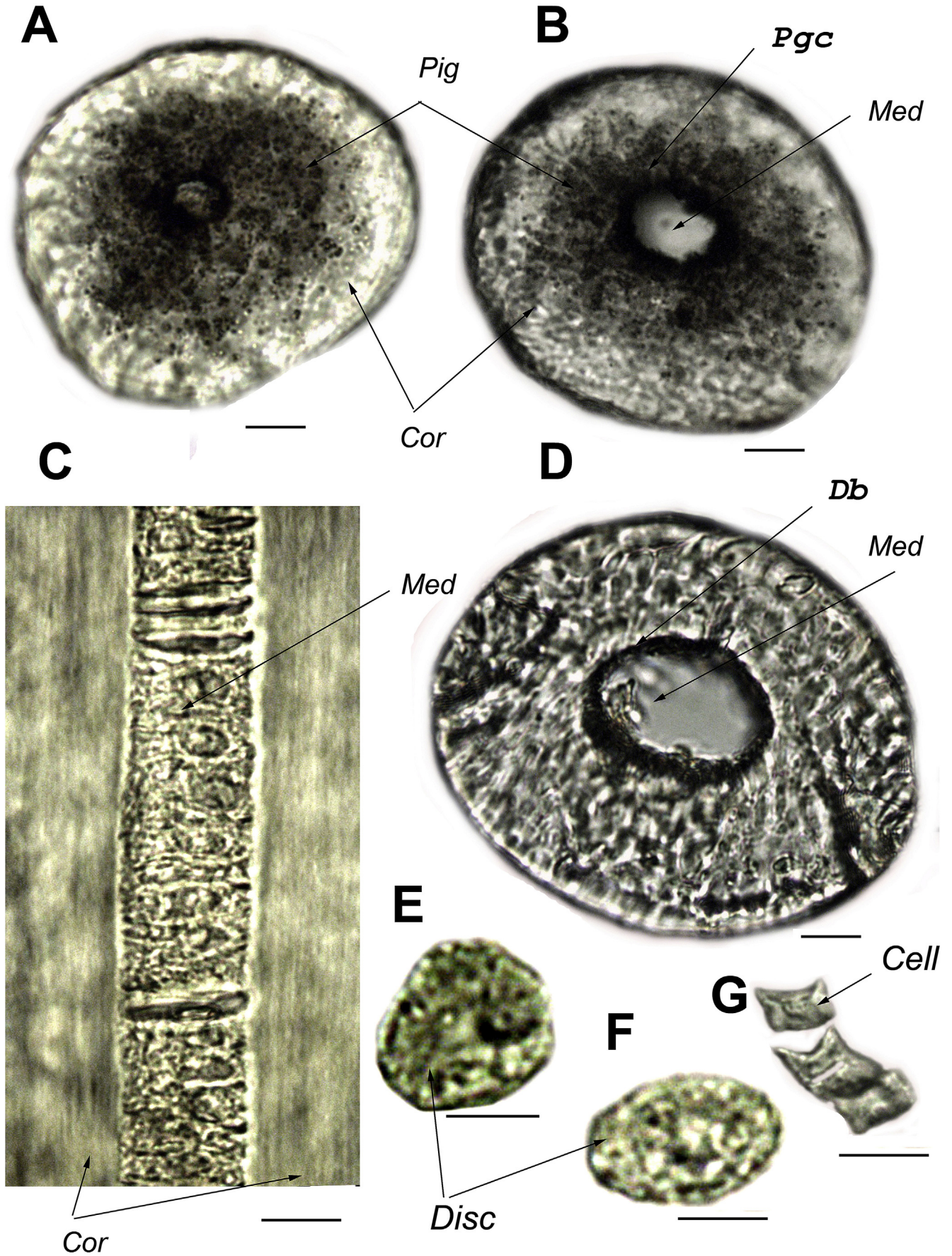
4.3.2. Microstructure of the cortex

4.3.2.1. The cave lion. The cortex of all hair categories is clearly separated from the medulla by a dark band that is wider at the base of the hair (Fig. 6A, B) than in the mid-length (Fig. 6D). The cortex is dense and more strongly pigmented around the medulla, and forms a dark ring on the periphery of the hair. Small pigment granules appear in clusters, which look like short strokes stretched along the shaft (Fig. 7 C). In SEM, the laminated structure of the cortex and the longitudinal slits are visible (Fig. 7A).

4.3.2.2. The African lion. In GH I, the boundary between the cortex and the medulla is clearly visible due to a dark band (Fig. 8A, B, D). The cortical layer is unevenly pigmented, ranging from small and scattered pigment granules to large clusters concentrated mainly in the median part of the shaft (Fig. 8B, D) and stretched along and across the shaft (Fig. 8C). Peripheral portions of the shaft are weakly pigmented and the dark band is absent. As in the cave lion hair, the cortex of the African lion hair has distinct longitudinal slits (Fig. 7B, C).

4.3.3. Microstructure of the medulla

4.3.3.1. The cave lion. In the GH, the boundary between the cortex and medulla is not smooth (Figs. 4A, B, C; 6A, B, D). The medulla is destroyed in many sections of the GH and DH but, where it remains, it has a lace-like appearance in which the entire mass of the medulla contains round cavities separated by partitions with numerous short-rimmed projections. These cavities are mostly small, but one large cavity is apparent (Figs. 5F; 6C; 7A). Sometimes the partitions separating the cavities appear flattened and extend in the form of polymorphic islands. In the medulla, many up to 1 μm long stick-like pigment granules are visible; these may represent 'spilled contents' of the destroyed medulla, which decomposes to the keratinous 'disks' during the process of thermal chemical hydrolysis. These disks are small in GH, with a diameter up to 20 μm , and they have improperly round or oval shapes (Fig. 6E, F). Clusters of pigment granules are unevenly distributed in the central part of the disks, but are more orderly on the disk periphery, where they form a nearly continuous, thin belt. During



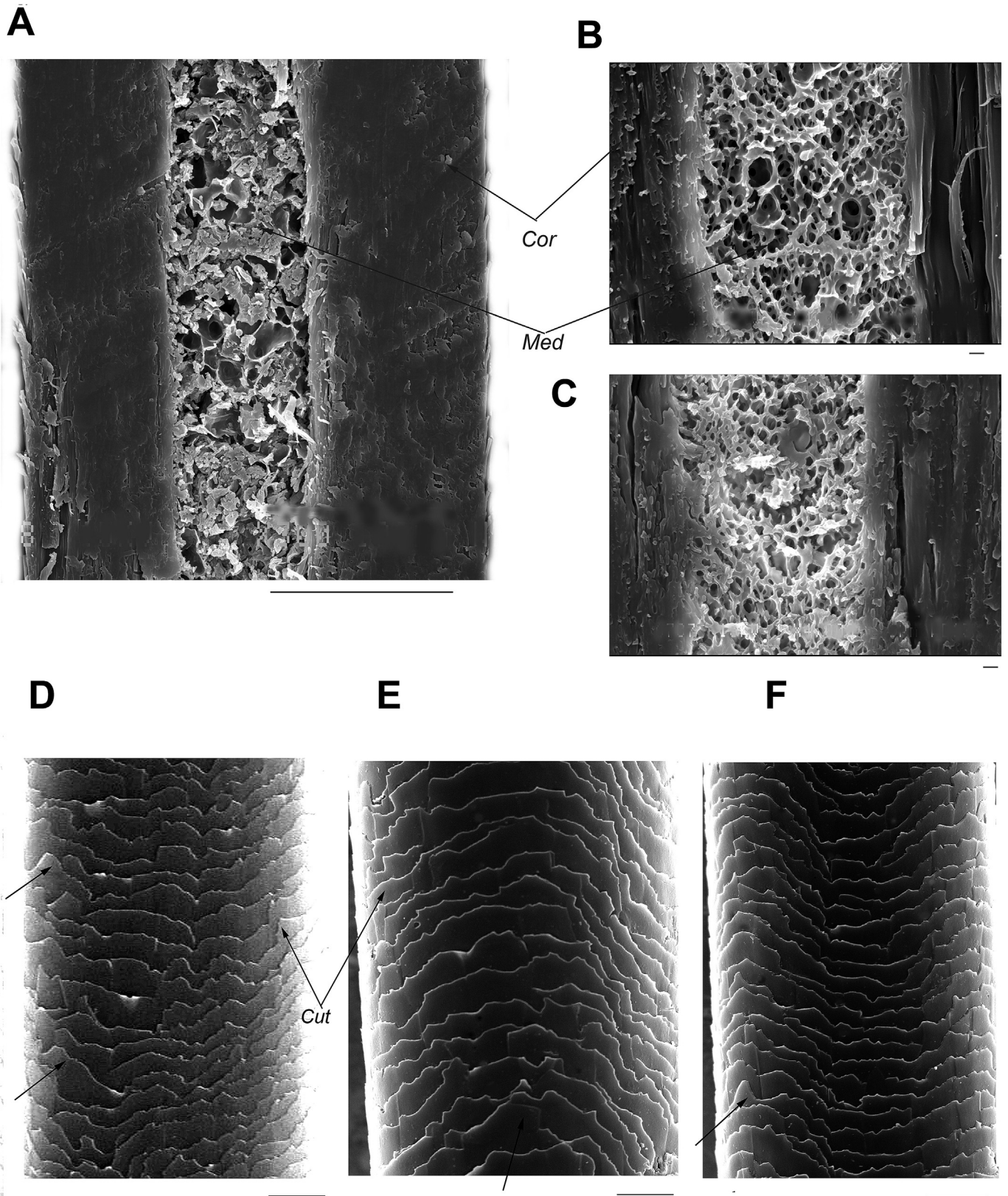
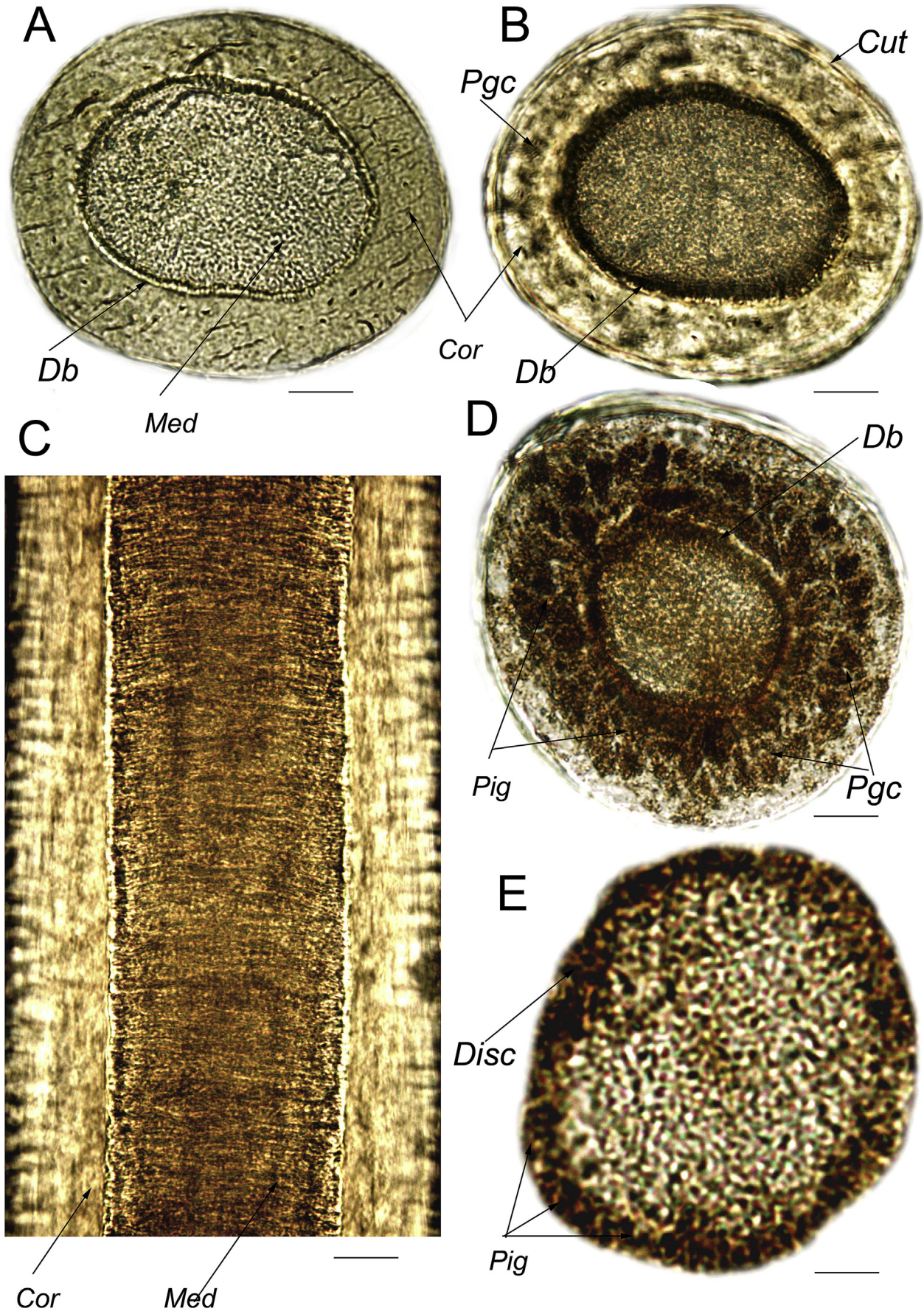


Fig. 7. SEM results showing microstructure of the cave lion guard hair (A, D) and the same of present-day African lion (B, C, E, F). (A, B, C) longitudinal sections of the hair shafts; (D, E, F) cuticular patterns on the outer surface of the hair; *Cor* = cortex; *Med* = medulla; the triangular ledges are shown by arrows. Scale bars are: A — 100 μm ; B, C — 1 μm ; D, E, F — 10 μm .

Fig. 6. Photomicrographs showing the microstructure of cave lion guard hair in cross section (A, B, D) and longitudinal section (C). (A) base of the shaft; (B) above the base of the shaft; (C, D) mid-length of the shaft; (E, F) medullar 'disk' macerated during earlier stages of thermo-chemical hydrolyses; (G) 'cells' of medullar disks macerated during later thermo-chemical hydrolyses; *Cell* = keratinous 'cell'; *Cor* = cortex; *Cut* = the cuticular scale; *Db* = the dark band between the cortex and medulla; *Disc* = keratinous disc; *Med* = medulla; *Pgc* = pigment granule clusters; *Pig* = pigment granules. Scale bars are 10 μm .



further maceration, disks become divided into individual 'cells', which are rectangular in shape but with outstretched corners in the form of horns (Fig. 6G).

4.3.3.2. The African lion. In the GH, the medulla is clearly separated from the cortical layer of the obvious pigmented band (Fig. 8A, B, D), and is delicate in structure (Figs. 4I; 7B, C; 8C). The medulla is similar to that of cave lion GH in that they contain rounded, mainly small cavities interspersed by large cavities (Fig. 4I). The walls of the cavities have short horn-like projections, and some are in a polymorphic flattened configuration. The configuration of the medullar disc is similar to that observed in cross section of the medullar canal: it is nearly round and with a dark peripheral dark ring (Fig. 8E). The disc is much bigger in African lion GH than in cave lion GH.

4.3.4. Surface ornament of the cuticle

4.3.4.1. The cave lion. The surface ornamentation (cuticular pattern) of the GH varies slightly along the shaft. In the base of the hair's cuticle is semi-ring (a scale that does not fully wrap around the shaft) and large scales with a gently curving free edge strictly strung across the shaft. The height of the scales reaches 10 μm . Higher up the shaft, the cuticle becomes rough and flat (a height of 4–8 μm), with a roughly broken free edge (Fig. 7D). Some scales lie at an angle of 30–40° to the transverse axis of the shaft. Even higher up the shaft, the cuticle remains roughly cut but the scales are larger, up to 15–20 μm . Some flakes have characteristic triangular ledges (Fig. 7D, arrows). Some scales with subtle folds are found throughout the shaft.

DH also have semi-ring cuticle (Fig. 5B, C). At the base of the shaft, scales are large (height up to 15 μm) and gently curved, but lack a free edge. Some scales lie at an angle of 35–40° to the transverse axis of the shaft. Above the shaft, some of the scales are slightly flattened and lie at an angle to the transverse axis of the shaft, and have rounded or roughly broken free edges. The ratio of the height of scale to the thickness of hairs (Index of cuticle, $n = 5$) is as follows: DH I shaft from the base to the mid-length: is 0.4 ± 0.03 ; GH I at the base of the shaft: 0.4 ± 0.05 ; GH I at mid-length of the shaft as the scales become flattened: 0.2 ± 0.06 ; GH I above the mid-length of the shaft as the scales again become high: 0.8 ± 0.01 .

4.3.4.2. The African lion. GH cuticles are thick, multi-layered, and semi-ringed. The ornamentation is similar to that of the cave lion. In the base of the shaft, the cuticle consists of flattened, slightly corrugated plates with a smooth free edge. Only a few scales lie at an angle of 40° to transverse axis of the shaft. Above the base, the shaft expands, has strongly flattened scales with a height not more than 10 μm in the mane and 5–8 μm in the back, and a highly indented edge with numerous triangular ledges (Fig. 7E, F). In the side of the shaft, many scales lie at an angle to the transverse axis of the shaft (Fig. 7E, right side). The index of cuticle in the mid-length of the shaft of mane GH is 0.1 ± 0.03 , and for GH of back GH is 0.08 ± 0.01 .

5. Discussion

Mitochondrial DNA analysis indicates that the hair sample studied falls within the diversity of Siberian cave lions (Ersmark et al., 2015), providing a clear taxonomic identification for the

hair samples. Previous work indicated that cave lions represent a lineage that became isolated from lions living today ~600 ky B.P. (Burger et al., 2004). Since this isolation, cave lions and their living cousins were subjected to very different environments, which likely resulted in the variety of differences observed when comparing their hairs.

Cave lion hair is distinct from that of living African lions in a variety of ways. The earliest lions are believed to have been maneless, with the maned form appearing only within the last several hundred thousand years (Yamaguchi et al., 2004). In addition, analyses of Paleolithic art suggest that male cave lions lacked a mane (Nagel et al., 2003). While no consensus has been reached as to the function of the lion's mane, hypotheses include heat conservation, social behavior, and protection during fighting (Kays and Patterson, 2002; Nagel et al., 2003). Males in some populations of the African lion, for example lions in Tsavo National Park in Kenya, lack a normally developed mane (Kays and Patterson, 2002). In these lion populations, a lack of mane has been associated with small pride size and the absence of strong competition between males (Kays and Patterson, 2002). Based on a lack of mitochondrial DNA diversity across the cave lion range, it is possible that cave lion communities were also small (Ersmark et al., 2015), and that this may have been associated with the lack of mane (Guthrie, 1990).

Our morphological analyses of the cave lion hair indicated that it was very diverse in both coloration and structure, and at least as diverse as the hair of present-day lions. The cave lion is distinguished from the present-day lion in that it had a thick and dense, downy undercoat composed of closely spaced and compressed, wavy, downy hair (DH) and slightly waved guard hair (GH III-IV). This arrangement of DH and GH and the well-developed medulla, which acts as a good thermal insulator, provides a thick, warm and flexible undercoat. Previously, we described a similar structure of fur and presence of wavy hair in the dense undercoat of an ancient bison, *Bison priscus* Bojanus, 1827 (Chernova and Kirillova, 2013). It is possible that the higher amount of differentiation and greater thickness of GH and increased abundance of compressed wavy DH, which we also observe here, and the twisted nature of cave lion GH compared to strait GH in modern lion, are common adaptations to conserve the body heat among large mammals living in glacial periods.

It is likely that the GH of the cave lion and the African lion provide mechanical defense of the undercoat, as all classes of GH have thick shafts. At the same time, GH also have good heat-insulating properties, based on good development of the medulla, and excellent hardness, based on the thick dorsal cortex due to the shifting of the medulla to the ventral side of the shaft and the rough and thick cuticle. These similar structural features may be the result of adaptation to different habitats: while the cave lion required protection from the cold, the African lion requires protection from overheating. A strong mechanical structure of the coat would also have been critical to both lion species, both for defense during fighting and hunting and for protection while moving quickly among grasses and bushes.

The morphometric features of the African lion hair studied here are not identical to those of the Asiatic lion that were reported previously (Chakraborty et al., 1996). For example, GH from the back of Asiatic lions varies in length from 17 to 48 mm and has a thickness of 70 μm (Chakraborty et al., 1996). These values are slightly smaller than those measured here (Table 4). Previous reports of the color, length and shaft configuration of Asiatic lion

Fig. 8. Photomicrographs showing the microstructure of the guard hair of present-day African lion on cross sections (A, B, D) and on longitudinal section (C) in mid-length of the shaft. (E) medulla 'disk' macerated during earlier stages of thermo-chemical hydrolyses; *Cor* = cortex; *Cut* = the cuticular scale; *Db* = the dark band between the cortex and medulla; *Med* = medulla; *Pgc* = pigment granule clusters; *Pig* = pigment. Scale bars are 10 μm .

mane hair (Chakraborty et al., 1996) are similar to those reported here, except for the narrow light band that we observed in the upper portion of the shaft, which goes into a black tip. While it is possible that these differences reflect variation among the lion subspecies, it is also possible that they also reflect individual variation, as results are reported from only single individuals.

Despite the potential variation among living lion subspecies, the cave lion hairs are distinct from both of these. In cave lions, neither the GH nor DH have a narrow light band on the upper half of the shaft (the GH and DH of the present-day lion do have such band), and many African lion GH I and II have black tips. Only GH III IV of the cave lion are bicolored: the lower half of the hair is dark and the upper part is light yellowish without a dark tip. The light ring in the African lion hair and light upper half of the cave lion hair may be remnants of coloration that was present in the common ancestor. The differences in the hair coloration are probably due to different conditions of lion habitat and the resulting differential evolution of camouflage capabilities.

The microstructures of the medulla and the cuticular pattern of cave lion hair are similar to those of the present-day lion and to other representatives of the genus *Panthera* Oken, 1816 (see Koppiker and Sabnis, 1976; Chakraborty et al., 1996; Chernova and Tselikova, 2004). This finding indirectly confirms the taxonomic affiliation of the cave lion to the genus *Panthera*. However, the height of the cuticular scales differs, with higher scales in cave lion hair than in African lion hair. This may indicate stronger mechanical properties of cave lion hair, which perhaps evolved as a consequence of the harsh and diverse habitat in which cave lions lived during the Pleistocene.

6. Conclusions

This first detailed analysis of preserved cave lion hair demonstrates that:

1. Cave lion hair is diverse and differentiated; we identified four orders of guard hair and two orders of downy hair, which is similar to that found in the present-day lion.
2. Unlike the present-day lion, cave lions had a very thick and dense downy undercoat, comprising dense, tightly woven, and compressed wavy downy hair and slightly wavy thinner guard hair, both with a well-developed medulla.
3. The coloration of cave lion hair is not similar to hair of the present-day lion, although there are some common features.
4. The microstructure and degree of development of the medulla and the cortex, and the ornamentation of the hair cuticle are similar in cave lions and present-day lions, but the cuticular scales are higher in cave lion hair.

Acknowledgments

We are grateful to the reviewers J Metcalfe and P Taru) for helpful comments during review, and to T.N. Tselikova and T.V. Perfilova for technical assistance. The study was supported by the National Alliance of Shidlovskiy “Ice Age” and the Russian Foundation for Basic Research (grant No. 15-04-08552). BS and AERS were funded in part by a grant from the Gordon and Betty Moore Foundation (grant No. GMBF3804).

References

Arduini, P., Teruzzi, G., 1993. *The MacDonal Encyclopedia of Fossils*. Little, Brown and Company, London.

Barnett, R., Shapiro, B., Barnes, I., Ho, S.Y.W., Burger, J., Yamaguchi, N., Higham, T.F.G., Baryshnikov, G., Boeskorov, G., 2001. The Pleistocene cave lion, *Panthera spelaea* (Carnivora, Felidae) from Yakutia, Russia. *Cranium* 18 (1), 7–23.

Bocherens, H., Drucker, D.G., Bonjean, D., Bridault, A., Conard, N.J., Cupillard, Ch., Germonpre, M., Honeisen, M., Munzel, S.C., Napierala, H., Patou-Mathis, M., Stephan, E., Uerpmann, H.-P., Ziegler, R., 2011. Isotopic evidence for dietary ecology of cave lion (*Panthera spelaea*) in North-Western Europe: prey choice, competition and implications for extinction. *Quat. Int.* 245, 249–261.

Burger, J., Rosendahl, W., Loreille, O., Hemmer, H., Eriksson, T., Götherström, A., Hiller, J., Collins, M.J., Wess, T., Alt, K.W., 2004. Molecular phylogeny of the extinct cave lion *Panthera leo spelaea*. *Mol. Phylogenet. Evol.* 30, 841–849.

Campos, P.F., Gilbert, T.M.P., 2012. DNA extraction from keratin and chitin. In: Shapiro, B., Hofreiter, M. (Eds.), *Ancient DNA: Methods and Protocols*, Methods in Molecular Biology 840. Humana Press, New York, NY, pp. 43–49.

Chakraborty, R., De, J.K., Chakraborty, S., 1996. Identification of dorsal guard hairs of Indian species of the genus *Panthera* Oken (Carnivore: Felidae). *Mammalia* 60 (3), 473–480.

Chernova, O.F., Tselikova, T.N., 2004. *Atlas volos mlekopitayushikh* (Atlas of the Mammal Hairs). KMK Scientific Press Ltd., Moscow (in Russian).

Chernova, O.F., Kirillova, I.V., 2013. Microstructura volos pozdnechetvertichnogo bizona Severo-Vostoka Rossii (hair microstructure of the late Quaternary bison from North-East Russia). In: (Proceedings of Zoological Institute, RAS, Leningrad 317(2), 202–216) *Trudy Zoologicheskogo Institute, Leningrad* (in Russian).

Chernova, O.F., Perfilova, T.V., Kiladze, A.B., Zhukova, F.A., Novikova, V.M., Marakova, T.M., 2011. Atlas microstructury volos mlekopitayushikh — ob'ektov biologicheskoi ekspertizy (Atlas of the Microstructure of Hairs of Mammals — Objects of Biological Expertise). Russian Federal Center of Forensic Science, Moscow (in Russian).

Dabney, J., Knapp, M., Glocke, I., Gansauge, M.T., Weihmann, A., Nickel, B., Valsiosera, C., Carcia, N., Pääbo, S., Arsuaga, J.L., Meyer, M., 2013. Complete mitochondrial genome sequence of a Middle Pleistocene cave bear reconstructed from ultrashort DNA fragments. *Proc. Natl. Acad. Sci. U. S. A.* 110 (39), 15758–15763.

Darriba, D., Taboada, G.L., Doallo, R., Posada, D., 2012. jModelTest 2: more models, new heuristics and parallel computing. *Nat. Methods* 9 (8), 772.

Diedrich, C.G., 2008. The holotypes of the upper Pleistocene *Crocota crocota spelaea* (Goldfuss, 1823: Hyaenidae) and *Panthera leo spelaea* (Goldfuss, 1810: Felidae) of the Zoolithen Cave hyena den (South Germany) and their palaeo-ecological interpretation. *Zool. J. Linn. Soc.* 154, 822–831.

Diedrich, C.G., 2011. The largest European lion *Panthera leo spelaea* (Goldfuss 1810) population from the Zoolithen Cave, Germany: specialized cave bear predators of Europe. *Hist. Biol.* 23 (2–3), 271–311.

Diedrich, C., Rathgeber, T., 2011. Late Pleistocene steppe lion *Panthera leo spelaea* (Goldfuss, 1810) skeleton remains of the Upper Rhine valley (SW Germany) and contribution to their palaeobiogeography, sexual dimorphism and habitus. *Hist. Biol.* 86, 1–28.

Edgar, R.C., 2004. MUSCLE: multiple sequence alignment with high accuracy and high throughput. *Nucleic Acids Res.* 32 (5), 1792–1797.

Ersmark, E., Orlando, L., Sandoval-Castellanos, E., Barnes, I., Barnett, R., Stuart, A., Lister, A., Dalén, L., 2015. Population demography and genetic diversity in the Pleistocene cave lion. *Open Quat.* 1, 1–14.

Fink, D., Hotchkis, M., Hua, Q., Jacobsen, G., Smith, A.M., Zoppi, U., Child, D., Mifsud, C., Gaast van der, H., Williams, A., Williams, M., 2004. The ANTARES AMS facility at ANSTO. *Nim. B* 223–224, 109–115.

Goldfuss, G.A., 1810. *Die Umgebungen von Muggendorf. Ein Taschenbuch für Freunde der Natur und Altertumskunde*. Erlangen. J. Palm. Nature; General; Nature/General; Social Science/Archaeology.

Gouy, M., Guindon, S., Gascuel, O., 2010. SeaView version 4: a multiplatform graphical user interface for sequence alignment and phylogenetic tree building. *Mol. Biol. Evol.* 27 (2), 221–224.

Guindon, S., Dufayard, J.F., Lefort, V., Anisimova, M., Hordijk, W., Gascuel, O., 2010. New algorithms and methods to estimate maximum-likelihood phylogenies: assessing the performance of PhyML 3.0. *Syst. Biol.* 59 (3), 307–321.

Guthrie, R.D., 1990. *Frozen Fauna of the Mammoth Steppe*. University of Chicago Press, Chicago, Ill.

Hua, Q., Jacobsen, G.E., Zoppi, U., Lawson, E.M., Williams, A.A., Smith, A.M., McMan, M.J., 2001. Progress in radiocarbon target preparation at the ANTARES AMS centre. *Radiocarbon* 43 (2a), 275–282.

Kays, R.W., Patterson, B.D., 2002. Mane variation in African lions and its social correlates. *Can. J. Zool.* 80, 471–478.

Kirillova, I.V., Tiunov, A.V., Levchenko, V.A., Chernova, O.F., Yudin, V.G., Bertuch, F., Shidlovskiy, F.K., 2015. On the discovery of a cave lion from the Maly Anyu river (Chukotka, Russia). *Quat. Sci. Rev.* 117, 135–151.

Kisin, M.V., 2001. *Sudebnaya biologicheskaya ekspertiza volos zhitovnykh* (The Forensic Biological Expertise of the Hairs of Animals). V. 2. The Russian Federal Center of Forensic Science, Moscow (in Russian).

Koppiker, B.R., Sabnis, J.H., 1976. Identification of hairs of some Indian mammals. *J. Bombay Nat. Hist. Soc.* 73, 5–20.

Kurten, B., 1985. The Pleistocene lion of Beringia. *Annu. Zool. Fenn.* 22, 117–121.

Meyer, M., Kircher, M., 2010. Illumina Sequencing Library preparation for Highly multiplexed Target Capture and Sequencing. *Cold Spring Harbor Protocols*, 6, pdb prot5448. Nauka, Moscow (in Russian).

Nagel, D., Hilsberg, S., Benesch, A., Scholz, J., 2003. Functional morphology and fur patterns in recent and fossil *Panthera* species. *Scr. Geol.* 126, 227–240.

O'Connell, T.C., Hedges, R.E.M., 1999. Isotopic comparison of hairs and bone: archaeological analyses. *J. Archaeol. Sci.* 26, 661–665.

Packer, C., Clottes, J., 2000. When lions ruled France. *Nat. Hist.* 109, 52–57.

Richardin, P., Gandolfo, N., Carminati, P., Walter, P., 2011. A new protocol for

- radiocarbon dating of hair and keratin type samples—application to an Andean mummy from the national museum of natural history in Paris. *Archaeol. Anthropol. Sci.* 3, 379–384.
- Shapiro, B., Hofreiter, M., 2012. Ancient DNA: methods and protocols. *Methods Mol. Biol.* 840.
- Sokolov, V.E., Skurat, L.N., Stepanova, L.V., Shabadash, S.A., 1988. *Rukovodstvo po izucheniyu kozhnogo pokrova mlekopitayushikh* (A Manual for the Study of Mammal Skin).
- Sotnikova, M., Nikolsky, P., 2006. Systematic position of the cave lion *Panthera spelaea* (Goldfuss) based on cranial and dental characters. *Quat. Int.* 142–143, 218–228.
- Turner, A., 1997. *The Big Cats and Their Fossil Relatives*. Columbia University Press. ISBN 0-231-10229-1.
- Vereshchagin, N.K., 1971. The Cave Lion and its History in the Holarctic and on the Territory of the U.S.S.R, vol. 49. *Trudy of Zoological Institute, Leningrad*, pp. 123–199 (in Russian).
- Wheeler, T., Rosendahl, W., Sher, A.V., Sotnikova, M., Kuznetsova, T., Baryshnikov, G.F., Martin, L.D., Harington, R., Burns, J.A., Cooper, A., 2009. Phylogeography of lions (*Panthera leo* ssp.) reveals three distinct taxa and a late Pleistocene reduction in genetic diversity. *Mol. Ecol.* 18, 1668–1677.
- Yamaguchi, N., Cooper, A., Werdelin, L., Macdonald, D.W., 2004. Evolution of the mane and group-living in the lion (*Panthera leo*): a review. *J. Zool. Lond.* 263, 329–342.